https://doi.org/10.5194/amt-2022-238
Preprint. Discussion started: 29 August 2022

Atmospheric Measurement Techniques Discussions

Validation of tropospheric ties at the test setup GNSS co-location site in Potsdam

Chaiyaporn Kitpracha[1,2], Robert Heinkelmann[2], Markus Ramatschi[2], Kyriakos Balidakis[3], Benjamin Männel[2], and Harald Schuh[1,2]

[1]Technische Universität Berlin, Chair of Satellite Geodesy, Kaiserin-Augusta-Allee 104-106, 10553 Berlin, Germany
[2]GFZ German Research Centre for Geosciences, Space Geodetic Techniques, Telegrafenberg, 14473 Potsdam, Germany
[3]GFZ German Research Centre for Geosciences, Earth System Modelling, Telegrafenberg, 14473 Potsdam, Germany

Correspondence: Chaiyaporn Kitpracha (chaiyaporn.kitpracha@gfz-potsdam.de)

Abstract. Atmospheric ties are the differences of atmospheric parameters between antennas or stations at the same site and meteorological conditions. However, there is often a discrepancy between the expected zenith delay differences and those estimated from geodetic analysis, potentially degrading a combined solution employing atmospheric ties to constrain atmospheric delay differences. To investigate the possible effects on GNSS atmospheric delay, this study set up an experiment with four co-located GNSS stations of the same type, both antenna and receiver. Specific height differences for each antenna w.r.t. one reference antenna have been measured. One antenna was equipped with a radome of the same height and type as an antenna close to the ground. Additionally, a meteorological sensor was used for meteorological data recording. The results show that tropospheric ties from the analytical equation based on meteorological data from Global Pressure and Temperature 3 (GPT3) model, Numerical Weather Models, in-situ measurements, and ray-traced tropospheric ties, reduced the bias of zenith delay roughly by 72%. However, the in-situ tropospheric ties yielded the best precision in this study. These results demonstrate that the instrument effects on GNSS zenith delays were mitigated using the same instrument. In contrast, although the effects of the radome on atmospheric delays are well known, the magnitude of the effects determined in this study is unexpectedly large. Additionally, multipath effects at low-elevation observations degraded the tropospheric gradients. To extract the instrument effect, we set up another experiment with three GNSS stations and four different antennas. The height differences between the three stations were on one centimeter level. One of the three stations could be adjusted in height to control the height displacement after changing antenna. We succeeded in keeping the shift in the GNSS zenith delays within 2 mm level. The bias on GNSS zenith delays and tropospheric gradients agrees with the result of the previous experiment in this study. Moreover, we successfully detected the antenna-dependent effect on both the GNSS zenith delays and gradients from this experiment.

https://doi.org/10.5194/amt-2022-238
Preprint. Discussion started: 29 August 2022

Atmospheric Measurement Techniques Discussions

1 Introduction

Over the past few years, many weather services have assimilated Global Navigation Satellite Systems (GNSS)-derived atmospheric delays into their forecast products (Dousa and Vaclavovic, 2014; Wilgan et al., 2022). The German Weather Service, Deutscher Wetterdienst (DWD), for example, assimilates slant wet delays, which describe water vapor variability above sites at a multitude of elevations and azimuths. Atmospheric water vapor and dry atmospheric gases refract the signals employed by GNSS, an effect that is quantified by the estimation of atmospheric delay coefficients (typically zenith delays and gradients) during the data analysis. The determination of Precipitable Water Vapor (PWV) with GNSS requires knowledge about the in-situ atmospheric pressure and temperature (c.f. Nilsson et al., 2013) because the data and models are accurate enough to allow for the assumption that the Zenith Wet Delays (ZWD) estimated from GNSS data analysis are related to what actually happens above a station in terms of water vapor content. The determination of atmospheric delays, however, is correlated with other parameters, most of all with the station height and the station clock, and can be affected by external circumstances, such as multipath signal and antenna-dependent biases. Our work contributes to the precise assessment of the quality of atmospheric delays from GNSS as an atmospheric measurement technique.

Since the signals employed using co-located space geodetic techniques, e.g., Very Long Baseline Interferometry (VLBI), GNSS, Doppler Orbitography and Radiopositioning Integrated by Satellite (DORIS), and Satellite Laser Ranging (SLR), are delayed owing to the same overlying atmosphere; estimates of that delay (zenith delays and gradients) can also be utilized to tie the techniques together, in addition to local and global ties. A strong correlation exists between atmospheric parameters, especially Zenith Tropospheric Delays (ZTD), and the height component (Schuh and Behrend, 2012). Therefore, an improvement in the ZTD estimation can theoretically improve the co-located station positions (Pollet et al., 2014). Thus, the atmospheric parameters at the same observing site (atmospheric ties) could improve the combination of space geodetic techniques to establish an ITRF meeting the GGOS goals (Plag et al., 2009; Männel et al., 2019). Moreover, an improvement in the ZTD estimation benefits the space geodetic techniques-derived PWV, which is essential information in climate studies. These benefits of atmospheric ties have been demonstrated in many studies, e.g. Krügel et al. (2007), Pollet et al. (2014), Hobiger and Otsubo (2014), etc. Typically, the ITRF and its quality depend on the assumed formal errors of ties, which are used to link space geodetic techniques (Ray and Altamimi, 2005). In this work, we investigate the formal errors of atmospheric ties via error propagation and empirically in terms of a comparison of various derivation methods. Moreover, the antenna-dependent errors are not relevant anymore because we mitigate these in the first experiment. However, they will be considered in the second experiment in this study. The condition for the correct application of the ties is that the ties are inserted in the equation system with appropriate formal errors. The major discrepancy between the estimated station coordinate difference and local ties are discontinuities in time series due to instrumental change, environmental effects, and local obstructions (Pinzón and Rothacher, 2018). Similar causes exist for atmospheric ties as well.

In the combination of space geodetic techniques, the combination process has been performed on the estimated parameters. Some parameters that are identical can be directly combined (e.g. EOP). However, for nonidentical parameters, such as station coordinates and tropospheric parameters, the relationship between the parameters must be provided (Rothacher et al., 2011). In

https://doi.org/10.5194/amt-2022-238
Preprint. Discussion started: 29 August 2022


Atmospheric Measurement Techniques Discussions

the case of station coordinates, the local ties can directly provide the relationship between the station coordinates of different stations at the co-location site. However, this might not be the case for tropospheric parameters since the estimated parameters might be defined differently depending on analysis center or software. For example, one might directly estimate the ZWD, whereas the others can estimate the correction of the ZTD. Therefore, one must be careful in applying ties for tropospheric parameters in the combination process.

Many studies have compared ZTD parameters at co-location sites from space geodetic techniques and Numerical Weather Models (NWM). Generally, these parameters have an agreement of better than 1 cm in the Root Mean Square (RMS) and are consistent with Numerical Weather Models and other meteorological measurements (Teke et al., 2011; Pollet et al., 2014). Teke et al. (2013) showed ZTD and gradients from CONT02 to CONT11 derived from observations of GNSS, VLBI, DORIS, Water Vapor Radiometers (WVR), and Numerical Weather Models. They found that the best agreement between VLBI and GNSS was roughly 5 to 6 mm at most co-location sites for the CONT02, CONT05, CONT08, and CONT11 campaigns. Additionally, they stated that the agreement and accuracy of the tropospheric parameters mainly depends on the humidity in the atmosphere. Pollet et al. (2014) also found that the consistency of ZTD parameters depends on the humidity level and the number of observations per estimated ZTD parameter. Heinkelmann et al. (2016) compared the atmospheric parameters derived by DORIS, GNSS, VLBI, and Numerical Weather Models at five co-located sites during CONT14. Moreover, they assessed ray-traced atmospheric parameters at different reference points at co-location sites. They discovered that the different reference positions caused a significant difference in ZTD, whereas the differences in gradients were less significant. They found that special weather events could introduce a large discrepancy in atmospheric parameters between space geodetic techniques. Also, DORIS determined less precise atmospheric parameters due to the relatively poor observation geometry. Kitpracha et al. (2020) analyzed the time series of the differences in atmospheric parameters at the Wettzell co-location site using three different GNSS observations (e.g., L1, L2, and the ionosphere-free linear combination of dual-frequency, L3) to estimate atmospheric parameters. They found that the instrumental changes caused significant jumps in the time series of the atmospheric parameters differences. Therefore, the impact of instrumental effects are needed to be investigated to improve the combination with tropospheric ties at GNSS intra-technique or inter-technique co-location sites.

We designed two GNSS co-location site experiments to investigate the potential instrumental effects on GNSS-derived atmospheric parameters in this study. With the first experiment (A20), we expect to learn what are the potential effects on GNSS-derived atmospheric parameters. Moreover, we designed this experiment to assess the quality of the tropospheric ties for each derivation method and the potential of applying tropospheric ties with sub-daily resolution. For the second experiment (A17), we demonstrate the impact of instrumental effects and calibrate the antenna-dependent effects on GNSS-derived atmospheric parameters. In Sect. 2.1, we describe both GNSS co-location experiments in detail. Sect. 3 discusses the GNSS data processing and the derivation of atmospheric ties from the analytical equations and ray-tracing through Numerical Weather Models. Sect. 4 discusses the compared results of GNSS-derived atmospheric parameters from both experiments. Finally, in Sect. 5, we summarize the results of the experiments.

https://doi.org/10.5194/amt-2022-238
Preprint. Discussion started: 29 August 2022


Atmospheric Measurement Techniques Discussions

2 GNSS co-location experiments

2.1 A20 rooftop experiment

We designed the GNSS co-location experiment to assess whether the expected atmospheric parameter differences that are calculated employing either in-situ meteorological observations or numerical weather model match those estimated from the independent geodetic analysis of data collected at these co-located stations. At any site, we expect from nodes of the same observing system a decreasing ZTD with increasing height at any given time. To prove this statement, we set up the experiment on the rooftop of the A20 building at Telegrafenberg, the campus of GFZ, Potsdam, Germany. This experiment utilized four Septentrio choke-ring antennas (IGS standard name: SEPCHOKE B3E6) and Septentrio PolaRx5 receivers. Figure 1 shows the setup of the experiment. We installed the antenna A201 at the highest place. A202 and A203 were placed lower than A201 with two meters and four meters height differences, respectively. Antenna A204 was placed on the same level as A203 but installed with a radome from Aeroantenna manufacturer (SPKE:SPECTRA PRECISION conical dome with spike; sold by Aeroantenna and NovAtel). Due to the fact that the radome induces some additional signal propagation delay on GNSS observations owing to its material and shape (Schmid, 2009), we expect it to increase the atmospheric zenith delays. A meteorological sensor (Vaisala WXT530) was installed to record air pressure, temperature, and relative humidity; the meteorological data logging interval was set to 300 s. The precision of the meteorological information can be found in Sect. 3.3. The horizontal separation was less than 15 m in this experiment, assuring that all GNSS antennas and the meteorological sensor were subjected to the same atmosphere condition. This experiment was conducted from 30th January to 7th March 2020. Additionally, we used this experiment to assess whether there is any benefit in applying tropospheric ties in sub-daily resolution (every hour in this study) with the analytical equation, NWM, and in-situ measurements for GNSS intra-technique combination.

2.2 A17 rooftop experiment

As various GNSS antennas are used in worldwide networks of the IGS, the error from the antenna types could differently show up in tropospheric parameters. Therefore, instrumental effects in GNSS-derived tropospheric parameters needs to be determined. For this purpose, we designed an experiment on the rooftop of the A17 building of GFZ Potsdam Telegrafenberg campus, Potsdam, Germany. The purpose of the second experiment was to quantify the instrumental effect of GNSS-derived tropospheric parameters. This experiment was conducted using three GNSS stations, two permanent GNSS stations, and one experimental GNSS station. The unique feature of this experiment is able to adjust the height of the antenna pole (see Fig. 2). The antenna pole is a steerable device that allows to alter the height of the antenna at a level of 10 cm. Thus, the heights of the reference point of the different antenna types are controlled to coincide at a level of a few millimeters. In other words, independent of the antenna type, the reference point positions agree after an initial phase where the antenna position is assessed and then adjusted according to the average height displacement estimated by a PPP. This special setup allows us to avoid any significant displacements between the tested antenna types, so that all changes in GNSS-derived tropospheric parameters can be attributed to instrumental effects.

https://doi.org/10.5194/amt-2022-238
Preprint. Discussion started: 29 August 2022

Atmospheric Measurement Techniques Discussions

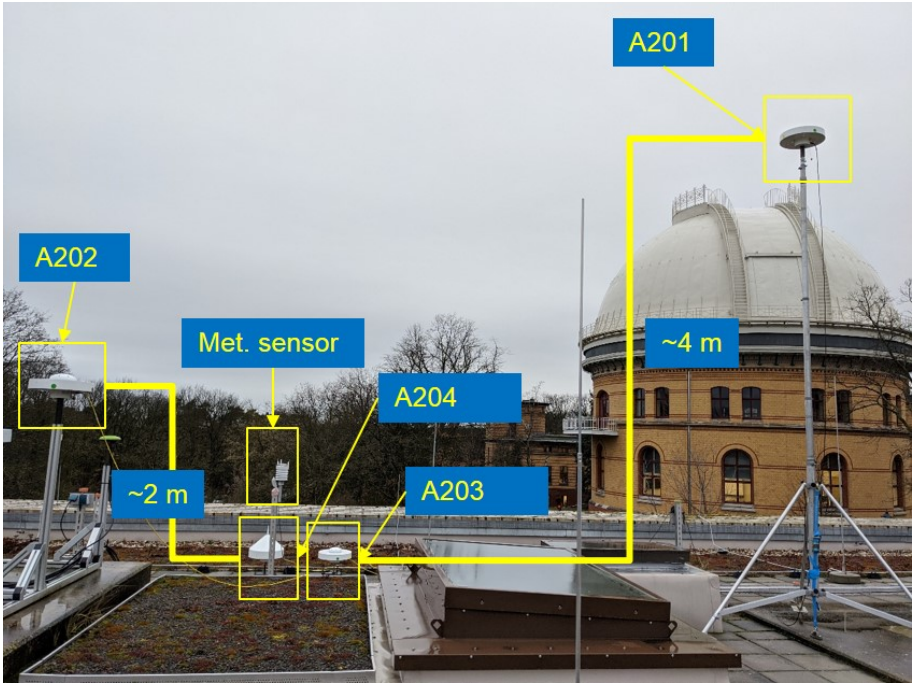

Figure 1. The GNSS co-location experiment set-up on the rooftop of A20 building (Telegrafenberg, Potsdam Germany). The antenna names, height differences, and meteorological sensor are shown.

GNSS observations at the experiment station were simultaneously collected with two different receivers; therefore, the experiment GNSS station names were given as A17F and A17G. This experiment involved two permanent GNSS stations from the IGS and GFZ networks, namely, POTS and POTM (Ramatschi et al., 2019), which are located on the rooftop of the A17 building. The distance between the three antennas were less than two meters in horizontal component and one decimeter for the vertical component. Five different GNSS antennas were employed sequentially in this experiment applying the above-mentioned "technical adjustment of the position, so that the reference points of all the antennas can be considered as not displaced". This specific set up is of high importance as we attempt to avoid effects on tropospheric parameters induced by different antenna positions. The effects might be caused, for example, by differences of multipathing or by different height of antenna reference points in the atmosphere typically cause tropospheric parameters to differ systematically. The list of equipment in this experiment is shown in Tab. 1. The experiment was conducted from 1st November 2021 to 10th January 2022.

https://doi.org/10.5194/amt-2022-238
Preprint. Discussion started: 29 August 2022

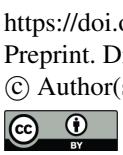

Atmospheric Measurement Techniques Discussions

Figure 2. Co-location experiment set-up on the rooftop of A17 building (Telegrafenberg, Potsdam Germany). The test station A17F/G was adjusted in such a way that the reference point positions of the various antennas did not show shifts within a few millimeters of tolerance. At the time when the photo was taken a JG5 antenna was installed on A17F/G (see Tab. 1). Meanwhile, two reference antennas were continuously operated that are part of the permanent IGS and GFZ networks named POTS and POTM equipped with JG5 and LR4 antennas, respectively.

https://doi.org/10.5194/amt-2022-238
Preprint. Discussion started: 29 August 2022

Atmospheric Measurement Techniques Discussions

Table 1. List of antennas in the A17 rooftop experiment. The designation of antenna follows the IGS standard name.

Station	antenna	radome	Abbreviation
POTM	LEIAR25.R4	LEIT	LR4
POTS	JAVRINGANT_G5T	NONE	JG5
A17F/G	JAVRINGANT_G5T	NONE	JG5
	LEIAR10	NONE	L10
	LEIAR20	NONE	L20
	JAV_GRANT-G3T	NONE	J3T
	SEPCHOKE_B3E6	NONE	SEP

3 Data analysis

3.1 GNSS processing

In this study, we analyzed GNSS observations using the Bernese GNSS software version 5.2 (Dach et al., 2015). Precise Point Positioning (PPP) approach was utilized based on CODE final orbit and clock information (Dach et al., 2020). The GNSS processing included the estimation of daily station coordinates, hourly zenith wet delays, and hourly horizontal gradients. The orbits are given in the IGS14 reference frame (Rebischung and Schmid, 2016), which is a GNSS-subset of the ITRF2014, and are consistent with the IERS Conventions 2010 (Petit and Luzum, 2010). The observation sampling rate was five minutes. Dual-frequency GPS and GLONASS code and carrier phase observations were applied to perform an ionosphere-free combination eliminating first-order ionospheric effects. The receiver clock parameters were estimated per observation sampling epoch. A priori ZHD was calculated based on grid model from the Vienna Mapping Function 1 (VMF1) (Böhm et al., 2006). The Vienna Mapping Function 1 (VMF1) was also applied to map the slant delays to zenith delays. The Chen and Herring (1997) model was utilized as the gradient mapping function. A cut-off elevation angle of seven degrees was applied and also elevation-dependent downweighting of observations following $1/\cos^2(z)$ where z is zenith angle.

3.2 Tropospheric ties of the A20 experiment

A difference in atmospheric parameters between GNSS antennas is expected due to the different antenna reference point locations in this experiment, primarily height differences. These can be called "tropospheric ties" (Teke et al., 2011; Heinkelmann et al., 2016). We determined tropospheric ties at the GNSS atmospheric parameter's estimation epochs with various methods and meteorological information and examined their performance. In this study, we defined tropospheric ties using an analytical equation from Teke et al. (2011) based on height differences and three different meteorological datasets, i.e., the Global Pressure Temperature model 3 (GPT3) (Landskron and Böhm, 2018) (T1), ERA5 NWM (Hersbach et al., 2020) (T2), and in-situ meteorological sensor (T3). We used the daily estimated coordinates as input for an analytical equation. The averaged coordinates over the entire campaign were used for extracting meteorological information from the NWM. The meteorological

https://doi.org/10.5194/amt-2022-238
Preprint. Discussion started: 29 August 2022

Atmospheric Measurement Techniques Discussions

information from the sensor was collected every 300 s and linearly interpolated to the estimation epoch. The pressure bias related to the height differences between the meteorological sensor and the GNSS reference point needs to be addressed. Thus, we corrected the pressure data from the meteorological sensor to each GNSS antenna reference point using an analytical equation from Teke et al. (2011). Moreover, tropospheric ties were determined from ERA5 NWM utilizing ray-tracing (Balidakis et al., 2018) (T4). The effect of horizontal distance was not investigated in this study because the expected gradient differences are well below the capability of the modern GNSS system, as described in Sect. 2.1.

Since the height is an essential information in tropospheric tie derivation, we investigated its precision in this study. The variations of the heights of the four antennas for the entire experiment were within 1 cm, as presented in Fig. 3. The standard deviations of height residuals were roughly 2 mm. This variation is expected because of many reasons, such as the building has some physical motion due to thermal expansion, satellite orbits and clock errors, and satellite's geometry during the day. However, this variation cannot affect the derivation of tropospheric ties significantly because the ZTD differences at the level of 1 mm require height differences at the level of 4 m due to the hydrostatic part (Bock et al., 2010).

Table 2 shows height differences and average tropospheric ties between the GNSS antennas from individual methods in this experiment. Tropospheric ties agreed very well between individual methods. This agrees with a previous study from Krügel et al. (2007). Additionally, the magnitude of the tropospheric ties increased with increasing height differences. Figure 4 shows hourly tropospheric ties between A201 and A203 stations during the experiment. The tropospheric ties from T2, T3, and T4 showed similar variability; however, tropospheric ties based on GPT3 showed almost no variation, which is expected given that GPT3 features only annual and semi-annual waves and the duration of the experiment was five weeks only. This shows that all tropospheric ties derivation methods account for the sub-daily atmosphere variation except T1, which contains only annual and semi-annual variations.

Table 2. Estimated height differences and mean tropospheric ties from individual methods, referring to the reference point of the individual GNSS reference antenna.

Station-pair		Height difference (m)	Mean zenith delay difference (mm)			
Ref.	Rov.		GPT3 (T1)	NWM (T2)	Met. Sensor (T3)	Ray-traced (T4)
A203	A204	-0.010	0.0	0.0	0.0	0.0
A202	A204	1.559	-0.5	-0.5	-0.5	-0.5
A202	A203	1.569	-0.5	-0.5	-0.5	-0.5
A201	A202	2.489	-0.8	-0.8	-0.8	-0.8
A201	A204	4.048	-1.2	-1.3	-1.2	-1.3
A201	A203	4.058	-1.2	-1.2	-1.2	-1.3

https://doi.org/10.5194/amt-2022-238
Preprint. Discussion started: 29 August 2022

Atmospheric Measurement Techniques Discussions

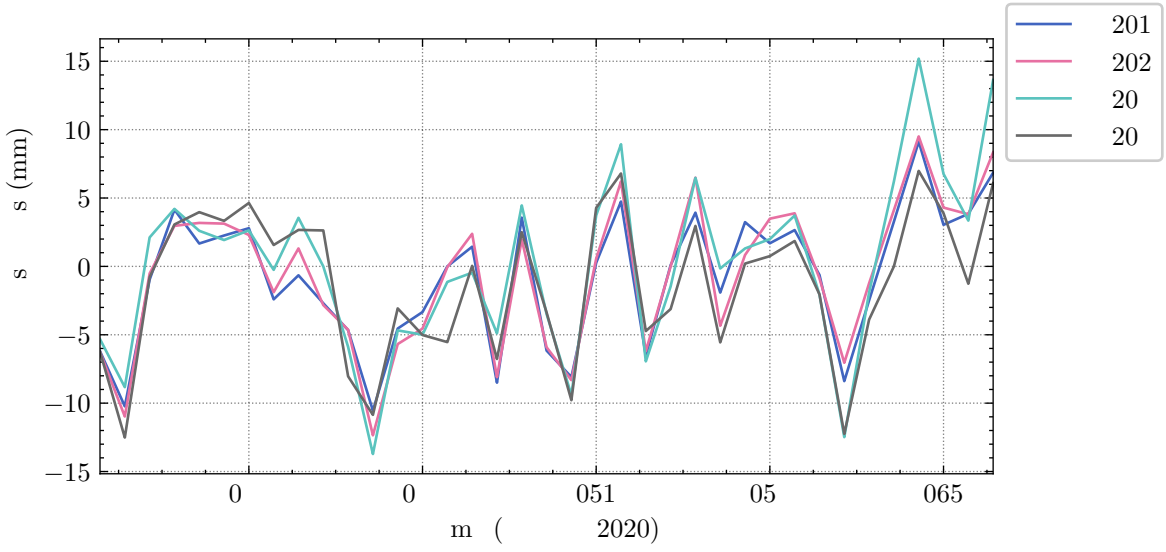

Figure 3. Residual height time series w.r.t mean values for the four antennas in the experiment.

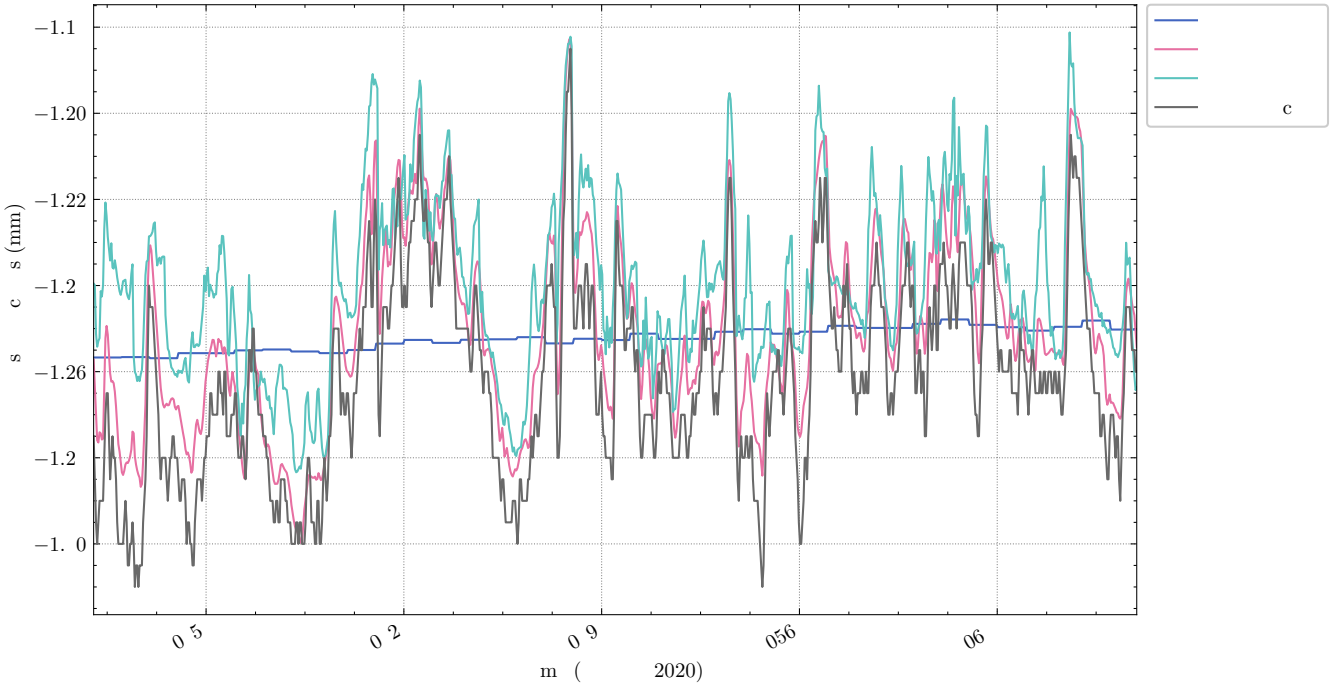

Figure 4. Zenith delay differences during the experiment between A201 and A203 stations (4 m height difference) from individual methods.

https://doi.org/10.5194/amt-2022-238
Preprint. Discussion started: 29 August 2022

Atmospheric Measurement Techniques Discussions

3.3 The uncertainties in meteorological parameters of the A20 experiment

The uncertainties of meteorological information, such as pressure, temperature, water vapor pressure, provided by GPT3, the meteorological sensor, and Numerical Weather Models, are described in Tab. 3. Unfortunately, the meteorological sensor cannot provide the water vapor pressure directly. For this study, we converted relative humidity to water vapor pressure using relative humidity and saturated water vapor pressure. We calculated the saturated water vapor pressure using the Magnus equation with coefficients from Alduchov and Eskridge (1996) and temperature from the meteorological sensor. Then, we performed error propagation to calculate uncertainties of water vapor pressure for the meteorological sensor at the estimation epoch.

Regarding the formal errors of NWM, we obtained the uncertainties from Balidakis (2019). However, these numbers are valid only for this experiment because the formal errors of NWM vary with location and time. Unfortunately, it is impossible to extract formal errors from GPT3 as this information is not provided. Therefore, we determined formal empirical errors of GPT3 by computing the differences w.r.t the meteorological sensor for each meteorological information. Then, the RMS of the differences was extracted. We applied these values as formal errors for GPT3. Therefore, these numbers are only valid for this experiment.

Table 3. The uncertainties of meteorological parameters from GPT3, ERA5 Numerical Weather Model, and the meteorological sensor (Vaisala WXT530) in the A20 experiment.

Parameters	Global Pressure Temperature 3	Numerical Weather Models	Meteorological sensor
Pressure (hPa)	10.8	1.0	0.5
Temperature (°C)	3.1	1.0	0.3
Relative Humidity (%)	n/a[a]	n/a[a]	3.0
Water Vapor Pressure (hPa)	1.0	1.0	0.3

[a]information is not available.

3.4 Data comparison

3.4.1 A20 experiment

We formed six pairs of GNSS stations in the experiment, as presented in Tab. 2. We calculated the weighted mean biases of the differences and the weighted root-mean-square (WRMS). Regarding ZTD comparison, we calculated five types of ZTD differences, following Table 4. Firstly, we calculated ZTD differences without applying tropospheric ties (S0). Secondly, we applied tropospheric ties using the analytical equation (Teke et al., 2011) based on meteorological information from GPT3 (S1), NWM (S2), and the meteorological sensor (S3), as well as ray-traced tropospheric ties (S4) before calculating ZTD differences to assess the performance of tropospheric ties from the individual methods. We performed error propagation from input parameters to calculate the uncertainty of tropospheric ties for each method. The uncertainties in meteorological parameters from GPT3, NWM, and the meteorological sensor can be found in Sect. 3.3. We also compared the tropospheric gradients and calculated

https://doi.org/10.5194/amt-2022-238
Preprint. Discussion started: 29 August 2022


Atmospheric Measurement Techniques Discussions

the time series of the differences between estimated gradients for each comparison case. Then, weighted mean biases, weighted standard deviation, and WRMS were calculated for each comparison case. As the GNSS antennas in this experiment observed the same tilt of the atmosphere, we expect no differences in the estimated gradients. Thus, we compared the estimated gradients directly without applying corrections.

According to Fig. 8, the observation geometry is similar for all antennas of the experiment. Therefore, the effects from observation geometry can be neglected in this study.

The cut-off elevation angle is a factor that affects GNSS-derived atmospheric parameter accuracy because the difference in number of observations and elevation angle-dependent errors contribute to the estimated GNSS-derived atmospheric parameters. Thus, this could affect the differences in GNSS-derived atmospheric parameters as well. Based on this, we briefly investigated the impact of using different elevation angles on the differences of ZTD and horizontal gradients by selecting two different cut-off elevation angles, such as seven and ten degrees, with the strategy described in Sect. 3.1. According to Fig. 5, the bias of estimated ZTD differences using seven degrees cut-off elevation angles was higher than the bias of using ten degrees cut-off elevation angle. Meanwhile, the bias of the estimated horizontal gradients of seven degrees cut-off elevation angle was less than using 10 degrees cut-off elevation angle. In contrast, the variations in the estimated ZTD and horizontal gradients differences using seven degree cut-off elevation angles were less than those using ten degrees cut-off elevation angle. This suggests that using high elevation angles reduces the impact of elevation-dependent systematic errors on the GNSS-derived ZTD differences. However, it increases the error in estimated horizontal gradients because the number of observations in the low-elevation angle, which is important for the horizontal gradients, is decreased. This finding agrees with a previous study by Ning and Elgered (2012).

3.4.2 A17 experiment

The A17 experiment consisted of two phases for each antenna following the first one. The first phase was to determine the differences in the reference point positions of the test antenna at A17F/G w.r.t. POTS/POTM. Firstly, we installed the JG5 antenna on A17F/G station. After six days of observation, we switched to the next antenna following the order in Tab. 1 and continued the same process for each antenna. Secondly, we processed the GNSS observations with the strategy described in Sect. 3.1. The time series of the height difference between A17F and POTS was calculated, and the average values were extracted for each test antenna. We determined the shift of the reference point position of the test antennas by comparing the mean difference values w.r.t. the mean difference of the JG5 antenna from the first observing period. In the second phase, we repeated the observing process and obtained tropospheric parameters. Between the phases, we vertically steered the antenna mount according to the shift value from the first phase. The time series of the height and tropospheric parameter (ZWD and horizontal gradients) differences between A17F/G and POTS/POTM were calculated. In this phase, we can assume that the change in the antenna reference point position does not exhibit significant effects on the tropospheric parameters differences.

In order to quantify the instrumental effects in GNSS-derived tropospheric parameters, we performed a double-differencing process. We took the mean difference of the JG5 antenna from the first observing period at A17F as the reference. We compared this with the mean differences of the other antennas at the same station in this experiment, including the JG5 antenna that

https://doi.org/10.5194/amt-2022-238
Preprint. Discussion started: 29 August 2022

Atmospheric Measurement Techniques Discussions

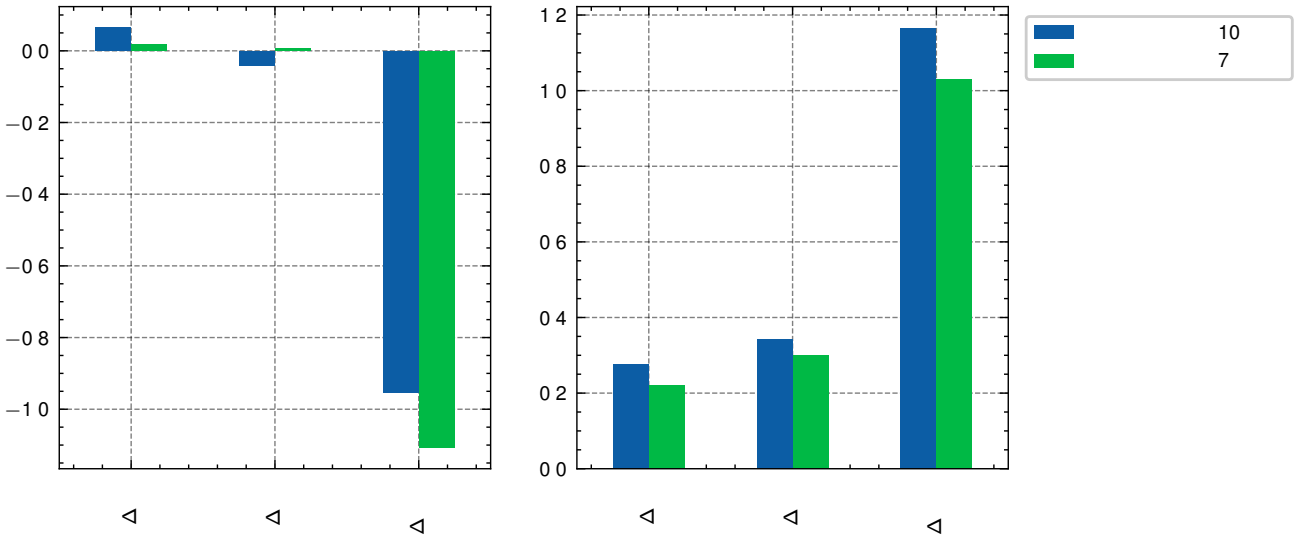

Figure 5. The impact of using different cut-off elevation angles on the differences of GNSS-derived atmospheric parameters between A201 and A202. Left and right figures show the weighted mean and the weighted standard deviation of the differences of the GNSS-derived atmospheric parameters, respectively.

observed again in the last period. With this approach, we expected that the systematic effects from the reference station would be eliminated. Therefore, the remaining biases are attributed to the instrument effect. This approach was utilized in the analysis of both ZWD and horizontal gradients in the A17 experiment.

Table 4. Description of ZTD comparison cases for the A17 experiment

Case	Tropospheric ties method	Meteorological data
S0	not applying ties	x
S1	analytical equation	GPT3
S2	analytical equation	NWM
S3	analytical equation	Meteorological sensor
S4	ray-tracing	NWM

https://doi.org/10.5194/amt-2022-238
Preprint. Discussion started: 29 August 2022

Atmospheric Measurement Techniques Discussions

4 Comparison of GNSS-derived atmospheric parameters

4.1 A20 experiment

4.1.1 ZTD comparison

We present a comparison of ZTD for each case described in Tab. 4. A selection of the results is provided in Fig. 6 and Tab. 5, while the complete set of results can be found in the electronic supplement.

Figure 6 shows the ZTD differences between A201 and A203 for all scenarios during the experiment. The bias between A201 and A203 for S0 was -1.5 mm, with an empirical standard deviation of 1.7 mm. Meanwhile, the biases for S1, S2, S3, and S4 were roughly -0.2 mm with a similar empirical standard deviation of S0 for all cases. This result shows that significant biases are mainly caused by height differences and atmospheric conditions. Moreover, tropospheric ties determined using the above-mentioned methods significantly reduced the biases. However, there was no improvement in the empirical standard deviation of the ZTD differences when applying tropospheric ties since the variation of tropospheric ties was less than 0.1 mm, as demonstrated in Fig. 4. This agrees with a previous study by Heinkelmann et al. (2016). According to Tab. 5, this situation also applied to the comparison between A201 and A202, A202 and A203. In contrast, we found an unexpected bias in the S0 case between A201 and A204. The bias was smaller than expected (less than 0.3 mm) despite roughly four meters of height difference that should result in a 1 mm bias. Thus, applying tropospheric ties increased the biases of ZTD differences, as shown in S1, S2, S3, and S4. These unexpected biases could also be seen when comparing A202 vs. A204, and A203 vs. A204. They are related to the radome, which has significant effects on the GNSS-derived atmospheric parameters. Therefore, installing a radome should be avoided unless necessary, as recommended in the IGS site guidelines (IGS, 2019).

Additionally, we calculated formal errors of tropospheric ties for the particular method in the experiment. The formal errors of T1, T2, T3, and T4 were 34.8, 3.2, 1.6, and 14.1 mm, respectively. T3 yielded the best precision in this study because the meteorological sensor provides high precision of the meteorological parameters, as presented in Sect. 3.3.

Table 5. Mean biases, standard deviation, and WRMS of the ZTD differences during the experiment for all cases. All values are in millimeters. The results are presented in weighted mean±weighted standard deviation (weighted root mean square) format.

Station-pair	S0	S1	S2	S3	S4
A201-A202	-1.10±1.03 (1.51)	-0.34±1.03 (1.09)	-0.34±1.02 (1.09)	-0.35±1.02 (1.09)	-0.33±1.02 (1.09)
A201-A203	-1.45±1.67 (2.22)	-0.20±1.67 (1.69)	-0.20±1.65 (1.67)	-0.22±1.63 (1.66)	-0.18±1.67 (1.68)
A201-A204	0.26±1.99 (2.10)	1.51±1.99 (2.50)	1.50±1.97 (2.48)	1.47±1.95 (2.44)	1.52±1.99 (2.50)
A202-A203	-0.35±1.69 (1.73)	0.14±1.69 (1.69)	0.14±1.68 (1.68)	0.15±1.67 (1.66)	0.13±1.69 (1.68)
A202-A204	1.37±2.02 (2.44)	1.85±2.02 (2.74)	1.84±2.01 (2.72)	1.82±2.00 (2.70)	1.85±2.02 (2.74)
A203-A204	1.70±2.25 (2.82)	1.70±1.25 (2.82)	1.70±1.23 (2.80)	1.69±1.21 (2.78)	1.70±1.25 (2.82)

https://doi.org/10.5194/amt-2022-238
Preprint. Discussion started: 29 August 2022

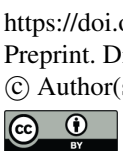

Atmospheric Measurement Techniques Discussions

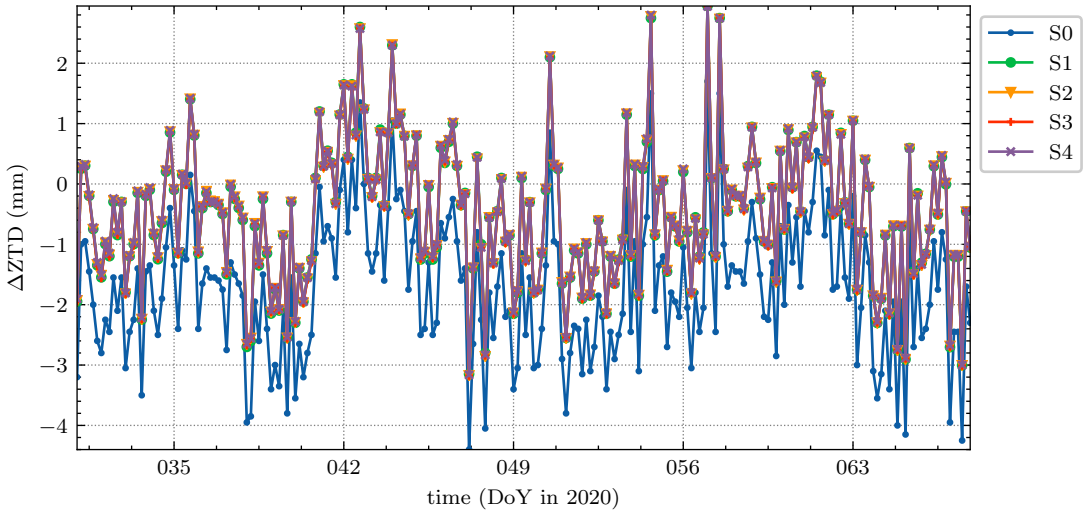

Figure 6. The ZTD differences (smoothed with a four-hours running median filter) between A201 and A203 for all case studies. The height difference is approximately four meters. S1, S2, S3, and S4 lines are relatively identical line because the means and variation are approximately equivalent, see Tab. 5.

4.1.2 Tropospheric horizontal gradients

In this section, we present a comparison of the tropospheric gradients. For each comparison case, we analyzed both north and east estimated gradients, as mentioned in Sect. 3.4.

Figure 7 shows the comparison of the estimated east gradients between the GNSS antennas during the experiment. The best agreement was found between A201 and A202. The bias and WRMS were 0.018 mm and 0.221 mm, respectively. These are expected because both antennas were installed horizontally close. In contrast, the biases were mostly between 0.1 and 0.2 mm, and the WRMS were at the level of 0.4 mm for the rest of the comparison. These results show that some effects degraded the estimated east gradients observed at A203 and A204. According to Fig. 1, some obstacles exist around A203 and A204, e.g., shadowing of refractor building, and the antennas were placed close to the ground. Therefore, there is a possibility of larger multipath effects for both antennas. According to Fig. 8, we found large residuals for low-elevation observations in A203 and A204, especially in the east-west direction. This shows that multipathing causes effects on the estimated east gradients in A203 and A204 antennas because the sensitivity of gradient estimates to low-elevation observations is much larger.

Additionally, the biases of the north gradient differences were at the level of 0.100 mm or better for all comparisons, see Tab. 6. The best agreement of the north gradients was found again for A201 and A202. The bias was 0.008 mm, and the WRMS was roughly 0.299 mm, whereas the WRMS for the rest of the differences was approximately 0.500 mm. This situation also similarly appeared in the east gradients. Therefore, multipathing also causes effects on the estimated north gradients. The north gradient biases were smaller than those of the east gradients in this experiment, except for the small difference between A201 and A202 because the residuals of north-south observations were smaller than the residuals of east-west observations, as shown

https://doi.org/10.5194/amt-2022-238
Preprint. Discussion started: 29 August 2022

Atmospheric Measurement Techniques Discussions

in Fig. 8. It is obvious that the north-south and east-west observations affect north-south and east-west gradient parameters, respectively. However, the WRMS of the north gradient differences were larger than the east gradient differences. According to Fig. 8, there are few observations in the northern part of the skyplot because of the inclination of the GNSS orbits. The deteriorated geometry might contribute to the high variation in the estimated north gradient.

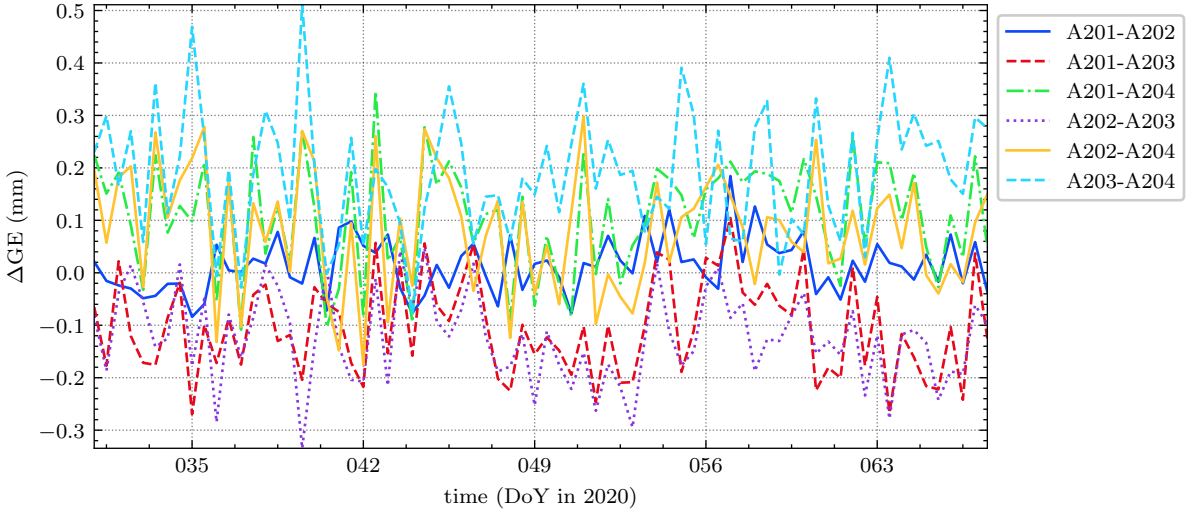

Figure 7. The differences of tropospheric east gradients (smoothed with a 12-hours running median filter) between the GNSS antennas in the experiment.

Table 6. Mean biases and WRMS of the tropospheric gradient differences from the experiment for all comparison cases.

Comparison cases	Differences of mean values (mm)		WRMS (mm)	
	East gradient	North gradient	East gradient	North gradient
A201-A202	0.018	0.008	0.221	0.299
A201-A203	-0.140	0.054	0.460	0.559
A201-A204	0.093	0.135	0.424	0.551
A202-A203	-0.158	0.052	0.449	0.553
A202-A204	0.076	0.132	0.413	0.572
A203-A204	0.229	0.082	0.532	0.561

https://doi.org/10.5194/amt-2022-238
Preprint. Discussion started: 29 August 2022

Atmospheric Measurement Techniques Discussions

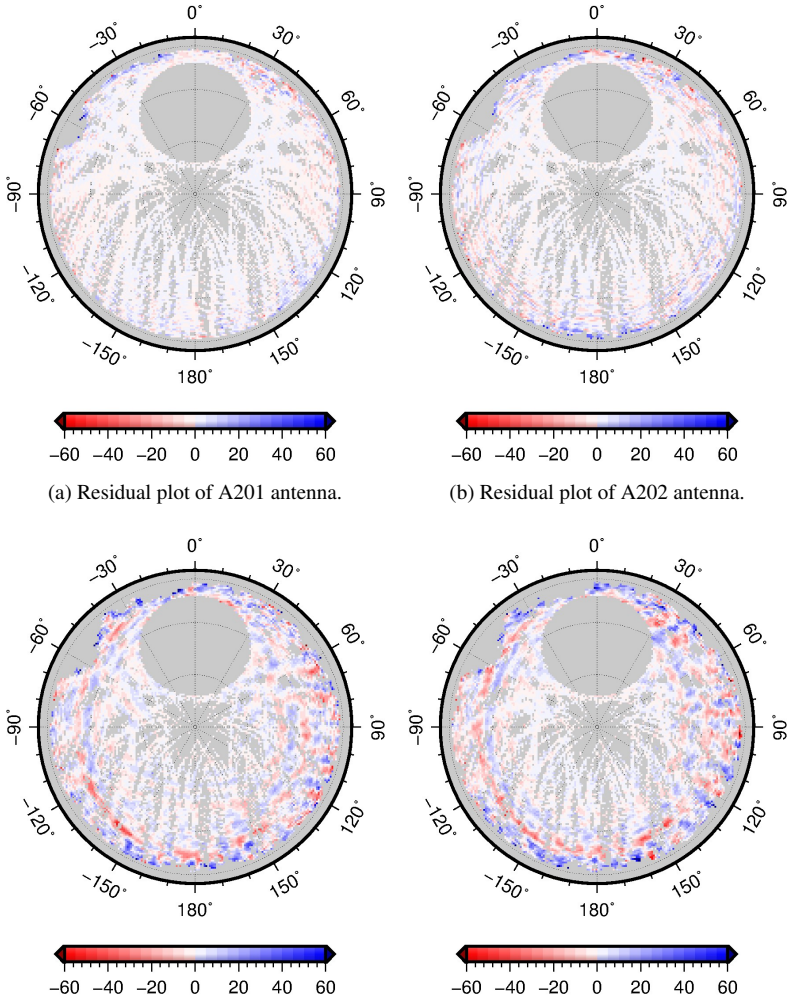

(a) Residual plot of A201 antenna.

(b) Residual plot of A202 antenna.

(c) Residual plot of A203 antenna.

(d) Residual plot of A204 antenna.

Figure 8. Residuals of ionosphere-free phase observations of A201, A202, A203, and A204 for the entire experiment. All units are in millimeters. A203 and A204 are the antennas that are mounted close to the roof, whereas the other two antennas are 2 m and 4 m, respectively above the floor of the rooftop. The skyplots demonstrate clearly that the large residuals of low elevation observations decrease with the height of the antenna above ground.

4.2 A17 experiment

In this section, we present the results of the A17 rooftop experiment. The results consist of the comparison of the ZWD parameters and the tropospheric gradients. Moreover, we show the instrumental bias in GNSS-derived atmospheric parameters extracted using the double-differencing process mentioned in Sect. 3.4.2.

https://doi.org/10.5194/amt-2022-238
Preprint. Discussion started: 29 August 2022

Atmospheric Measurement Techniques Discussions

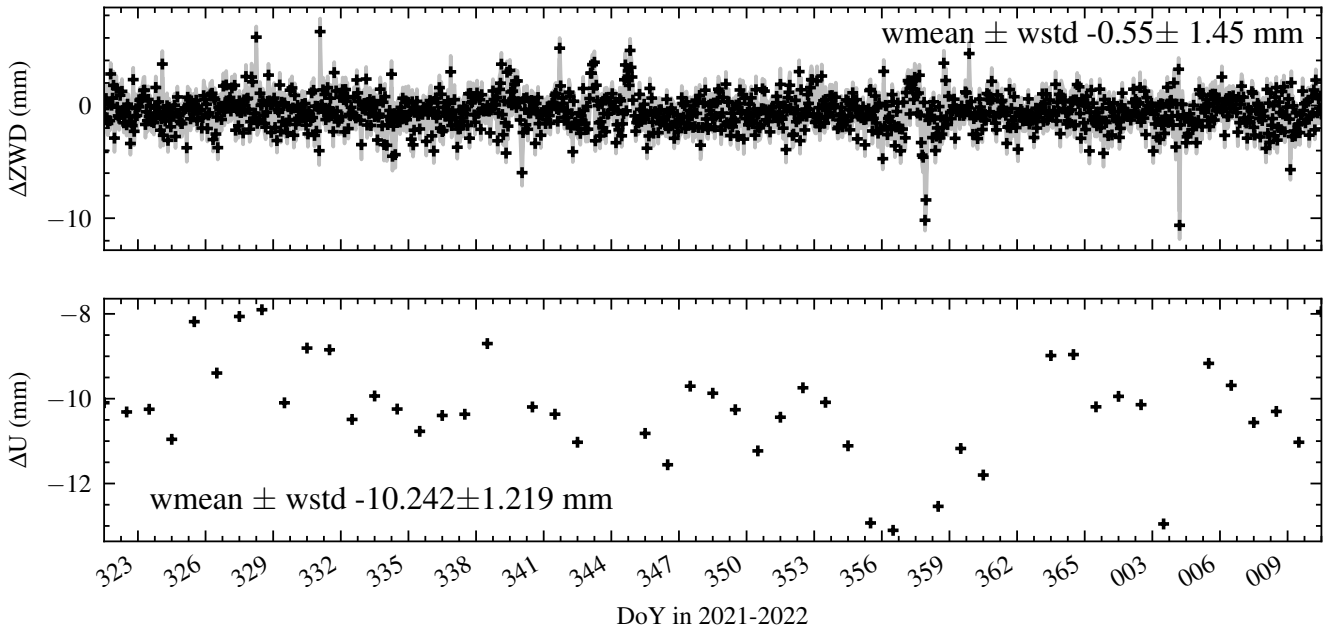

Figure 9. The comparison of ZWD parameters and up component between the POTS and POTM. Statistics values (weighted mean (wmean) and standard deviation (wstd)) are shown for both parameters.

Figure 9 shows a comparison between POTS and POTM, which are the reference stations in this experiment. The bias and standard deviation of ZWD differences were -0.56 and 1.29 mm, respectively. This result agrees with the results from the A20 experiment where the height difference between two antennas was less than one meter and using a different instrument. According to Fig. 10, the average height differences of A17F/G w.r.t. reference stations (POTM/POTS) for each antenna approximately agreed at the 2 mm level. These results show the success of steering the reference point positions, which is the target of the A17 experiment. The J3T antenna was not considered in this study because we could not control the average height difference in the J3T to agree within two millimeters with the rest antennas. Figure 11 shows the comparison of ZWD parameters as well as height differences of the test antenna w.r.t the reference stations. The results show that there were shifts in the time series of ZWD differences, whereas the shifts in the height difference time series were negligible. This demonstrates that the shift in the ZWD difference time series was not affected by changing reference position. It is likely that the different bias for each experiment antenna was caused by the instrumental effect. Moreover, severe weather events (heavy rainstorm) occurred in the L20 and SEP antennas. These clearly affected the biases of ZWD differences as well. The JG5 antenna in two different periods showed similar mean biases, according to Fig. 12. This demonstrates that the instrument effect in GNSS-derived tropospheric parameters is probably time-independent. However, the insignificant difference was due to the different weather conditions between the two observation periods.

https://doi.org/10.5194/amt-2022-238
Preprint. Discussion started: 29 August 2022

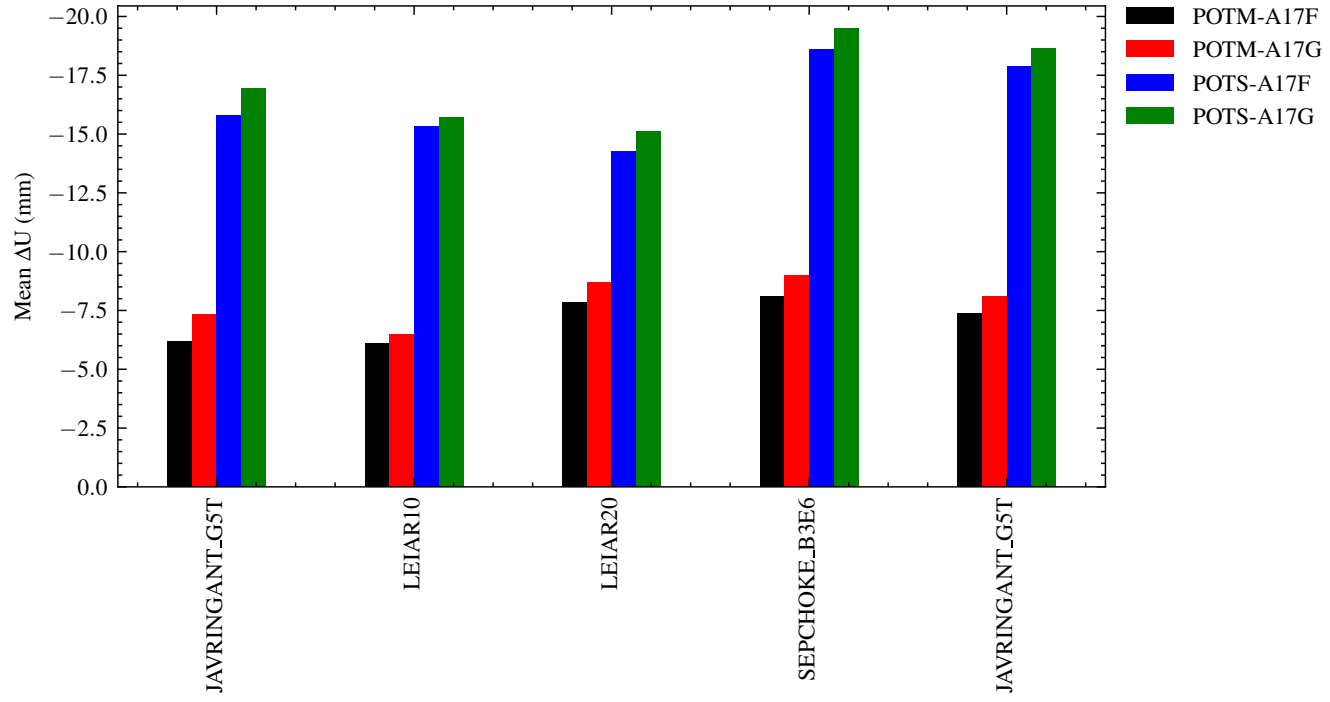

Figure 10. The mean height differences between A17F/G stations and two reference stations (POTM/POTS) for each individual antenna.

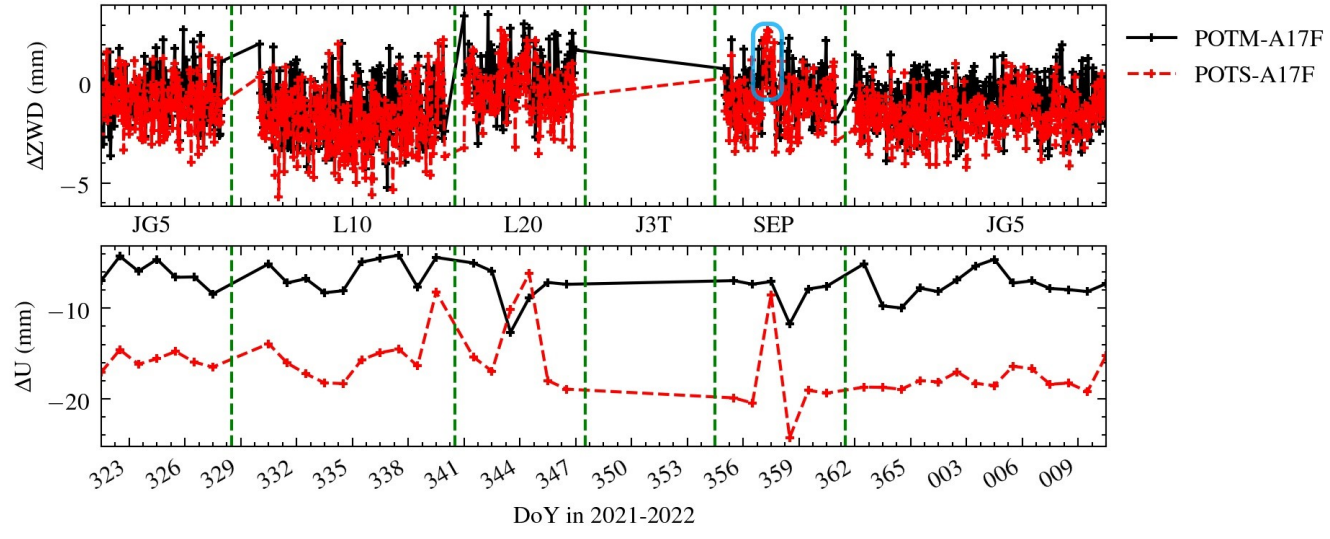

Figure 11. The ZWD parameters comparison w.r.t. reference station for the A17 rooftop experiment, as well as the height differences. Abbreviations of the test antenna types are given between the plot. The J3T antenna was skipped due to the unsuccessful steering reference point position. Green dashed lines indicate an antenna change. Light blue rectangle indicates the severe weather event.

https://doi.org/10.5194/amt-2022-238
Preprint. Discussion started: 29 August 2022

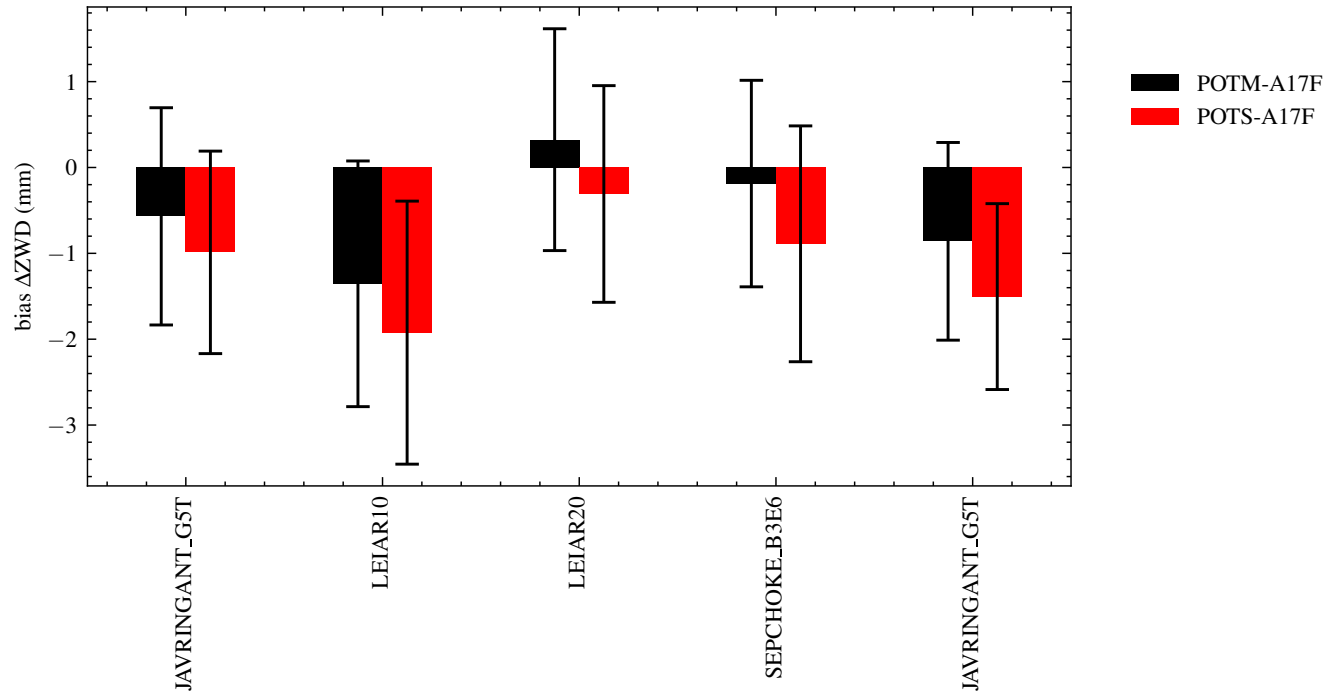

Figure 12. The average ZWD differences between the A17F station and the two reference stations (POTM/POTS) for the individual antennas.

We also performed a comparison of tropospheric gradients. Figure 13 shows the mean of the tropospheric gradient differences between A17F and POTS/M for the individual test antennas. Similar to the ZWD comparison results, the biases in tropospheric horizontal gradients were different for an individual antenna. The biases of east gradient differences were larger than those of north gradients. These were where multipathing occurred in the low-elevation observations of the test station, as shown in Fig. 14. The JG5 antenna also showed similar biases for two different observing periods, similar to ZWD parameters. These prove that the instrumental effect occurs in both parameters, GNSS-derived ZWD and gradients.

To extract the instrumental biases, we performed double-differencing as described in Sect. 3.4.2. Figure 15 shows the double-differenced ZWD biases for A17F/G w.r.t. POTS/POTM stations. The potential biases from the reference stations are supposed to cancel during the double-difference process. Therefore, these biases reflect the instrumental bias in GNSS-derived atmospheric parameters. As mentioned previously, we expect the same bias for the same instrument. However, a small bias remains in the JG5 antenna. Similar findings were also obtained for tropospheric gradients.

5 Conclusions

This study investigates the systematic effects of GNSS-derived atmospheric parameters and the performance of tropospheric ties by setting up two GNSS co-location site experiments. According to the A20 rooftop experiment results, the application

https://doi.org/10.5194/amt-2022-238
Preprint. Discussion started: 29 August 2022

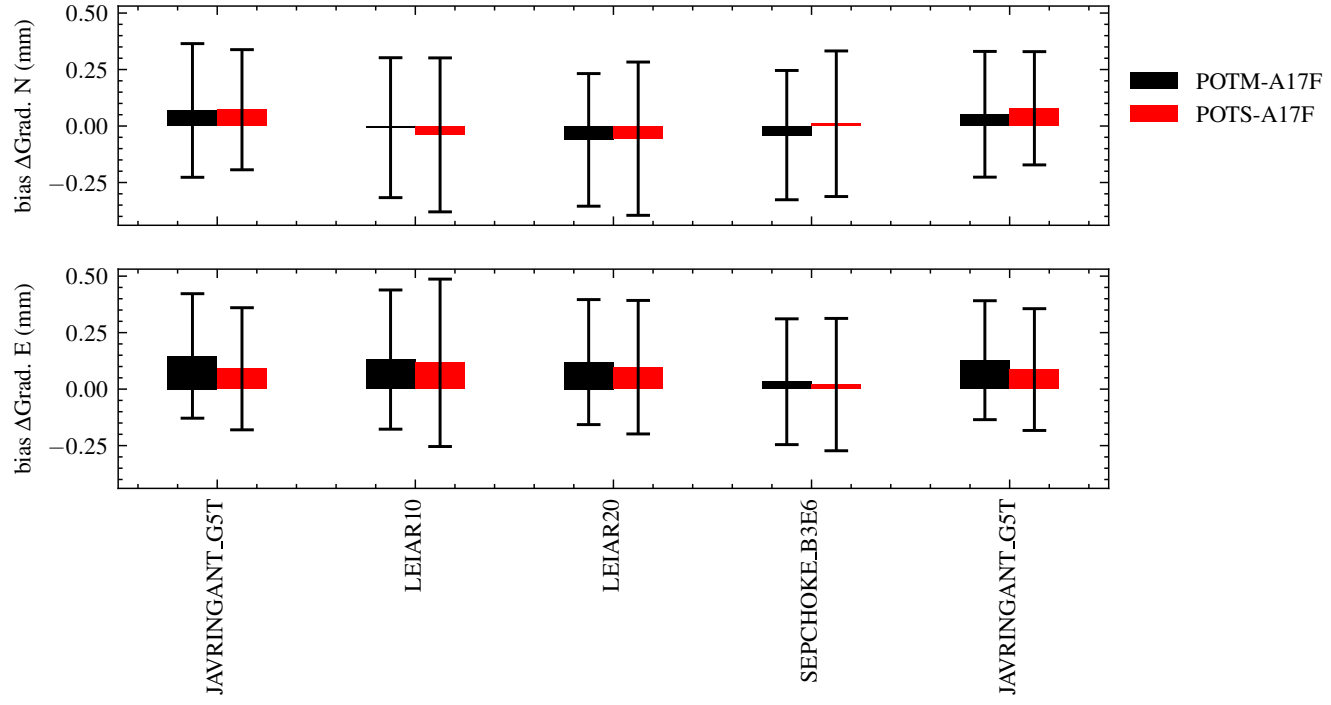

Figure 13. The average of tropospheric horizontal gradient differences between the A17F station and the two reference stations (POTM/POTS) for the individual antennas.

of tropospheric ties on ZTD decreases the mean differences between the antennas by 72%, i.e., from -1.7 mm to -0.5 mm, while the standard deviations remain unaffected for small height differences. These results confirm that the ZTD bias between antennas depends only on height differences and atmospheric conditions if using the same instrument at a co-location site. Moreover, applying tropospheric ties in sub-daily resolution shows insignificant improvements for small height differences, as presented in this study. Nevertheless, the radome causes an additional effect on the GNSS measurements. For the determination of atmospheric parameters, we can confirm that installing radome should be avoided, as recommended by the IGS site guidelines (IGS, 2019). Additionally, tropospheric ties from analytical equations with meteorological data from the standard model, Numerical Weather Models, in-situ measurements, and ray-traced tropospheric ties show similar performance for small height differences between GNSS antennas. One should mention that this result cannot be generalized neither to other geographical positions nor to cases where larger height differences are present. Nevertheless, tropospheric ties from an analytical equation based on in-situ measurements show the best precision in this study as assessed by formal errors and confirmed by the statistics determined empirically. Therefore, a meteorological sensor should be operated along with the GNSS station even at co-locations that involve small vertical distances. However, if a meteorological sensor is not available, the Numerical Weather Models can be another option in tropospheric ties determination in particular because of the ray-tracing that can be done through the weather model fields.

https://doi.org/10.5194/amt-2022-238
Preprint. Discussion started: 29 August 2022

Atmospheric Measurement Techniques Discussions

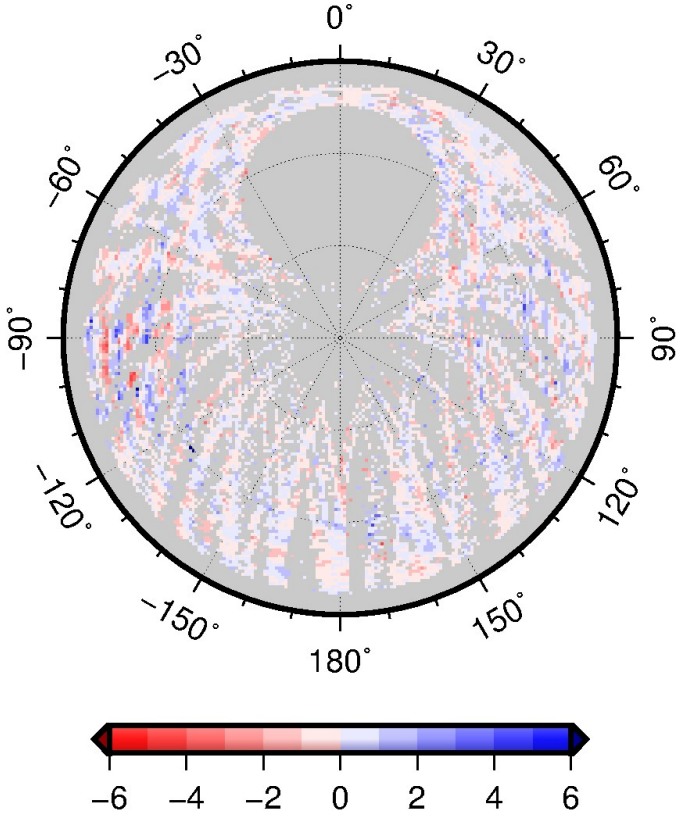

Figure 14. Residuals of ionosphere-free phase observations of A17F for the first observing period of the JG5 antenna. The unit is in millimeters.

The best agreement of tropospheric gradients was found between A201 and A202, which was expected. However, the multipath effects on low-elevation observations degrade the agreement of tropospheric gradients from GNSS in this study. Therefore, the GNSS antenna should not be installed close to the ground or in the vicinity of an obstacle that causes multipath signals, as recommended by the IGS site guidelines (IGS, 2019). Moreover, lacking observations in the northern part of the sky limited through the orbit inclination caused a larger variation in the north gradients compared to the east gradients in the A20 rooftop experiment.

In the A17 rooftop experiment, we successfully minimized the height shift during antenna changing within millimeter level. Additionally, the height difference between the reference station and experiment station was on one centimeter level. According to the A20 rooftop experiment, this number was not significantly affected in observed tropospheric ties. Moreover, the bias due to the height shift was insignificant. However, the severe weather event caused a shift in the GNSS-derived atmospheric parameters time series. Therefore, we conclude that the biases on observed tropospheric ties reflect the instrumental biases on GNSS-derived atmospheric parameters, if no severe weather event happens. We also succeeded in extracting the instrumen-

https://doi.org/10.5194/amt-2022-238
Preprint. Discussion started: 29 August 2022

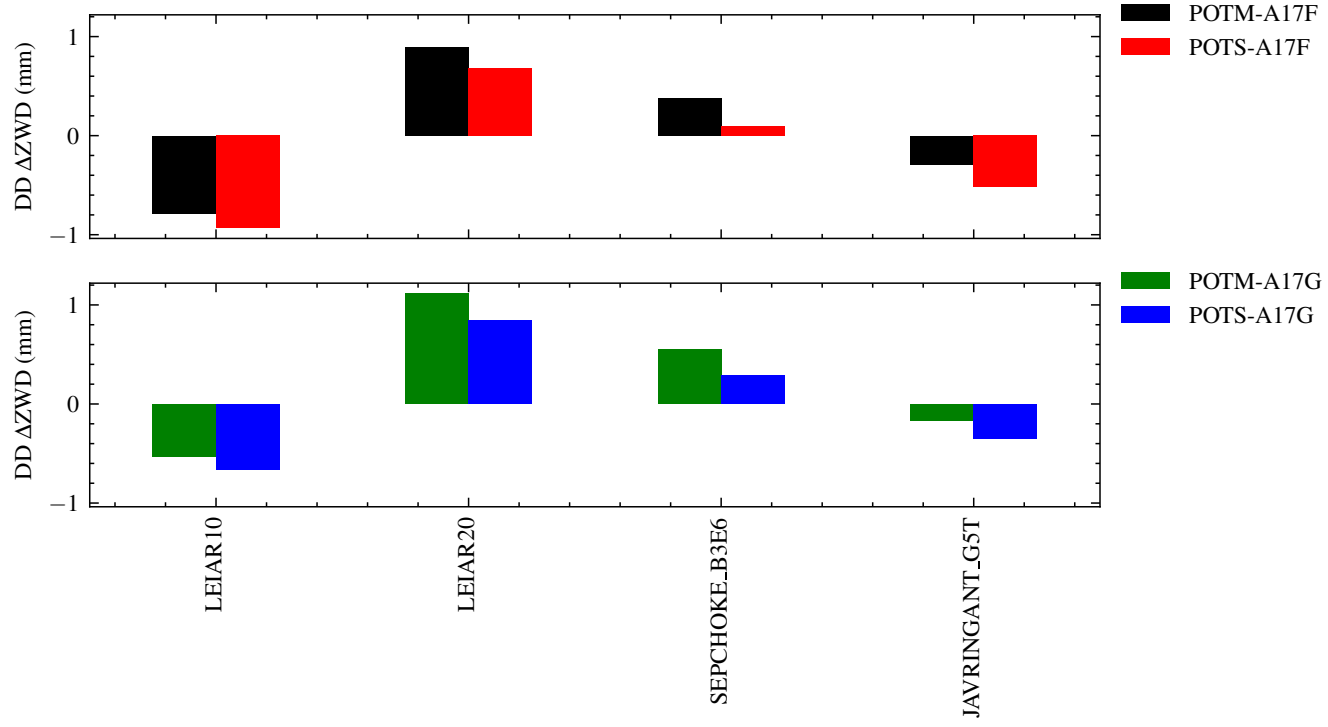

Figure 15. The antenna-dependent biases of ZWD extracted from the double-differencing process for A17F/G w.r.t. two reference stations (POTS/POTM). As these are derived in the sense of closed loops, one would expect zero for all the cases.

tal bias on GNSS-derived atmospheric parameters from this experiment using double-differencing process, despite that the instrumental biases for the same antenna (JG5) were slightly different at different observing period.

The technique-dependent systematic effects, such as radome and multipath effects, are considered the primary source of biases of the GNSS-derived atmospheric parameters in this study. This statement agrees with previous findings from Steigenberger et al. (2013) that showed multipath effects and radome-induced biases in the estimated coordinates that simultaneously affect ZTD parameters. Systematic errors due to uncalibrated radome and multipathing need to be avoided as they impose the thread of introducing noise-like and systematic errors that can be at the size or even larger than the tropospheric ties for the zenith delays. Therefore, these effects need to be avoided, especially multipath effects, to determine precise ZWD parameters from GNSS, necessary for Precipitable Water Vapor determination for climate studies. In this dedicated best case study, four tropospheric ties models perform comparably well as corrections due to height difference. From this experiment, there is no clear preference for one of the tropospheric ties models. Another potential systematic error source of the zenith delays is the instrumental bias when operating different antenna types. This error source was investigated in this study and successfully determined. The gradients are even more vulnerable. Since they are small, typically at the sub-mm level, the small systematic effects, e.g., due to multipathing, have a larger effect on them, relatively. With the application of the tropospheric delay model,

https://doi.org/10.5194/amt-2022-238
Preprint. Discussion started: 29 August 2022


Atmospheric Measurement Techniques Discussions

however, the values of the gradients get amplified, and thereby they can have significant effects on the refraction model and consequently on other parameter groups. Concluding, although the gradients do not require a height-dependent correction for small height differences, such as the tropospheric ties for the zenith delays, they can be affected by systematic errors more significantly than the zenith delays. Hence, it is questionable whether gradients can provide an accurate way of inter-technique combination. In comparison to zenith delays, the parameterization of gradients a longer time intervals should be applied.

Further investigation is required as both experiments were conducted only for a short period of about five weeks and a single dedicated site. Additional effects could occur in a long time series of GNSS-derived atmospheric parameters. Moreover, increasing the distances (both horizontal and vertical) between the GNSS antennas could determine how much the errors of the atmospheric parameters depend on distance or at least, the limitation of the application of tropospheric ties in the combination of atmospheric parameters.

Data availability. The datasets obtained for the experiments are available upon request from the corresponding author.

Author contributions. CK did most of the data analysis and writing of the manuscript. CK, RH, and MR participated in the design of the experiment and helped to improve the manuscript. KB, BM, and HS contributed to discussion of the results and improving the manuscript. All the authors read and approved the final manuscript.

Competing interests. The authors declare that they have no conflict of interest.

Acknowledgements. We would like to thank to Deutscher Akademischer Austauschdienst (DAAD) for financial support by granting scholarship to the main author under grant number 91650950. We also would like to thank Mr. Thomas Gerber for kindly helping us to set up the experiment. KB acknowledges funding from Deutscher Forschungsgemeinschaft (DFG, German Research Foundation) – Project-ID 434617780 – SFB 1464 (TerraQ).

https://doi.org/10.5194/amt-2022-238
Preprint. Discussion started: 29 August 2022

Atmospheric Measurement Techniques Discussions

References

Alduchov, O. A. and Eskridge, R. E.: Improved Magnus form approximation of saturation vapor pressure, J APPL METEOROL, 35, 601–609, 1996.

Balidakis, K.: On the development and impact of propagation delay and geophysical loading on space geodetic technique data analysis, Doctoral thesis, Technische Universität Berlin, Berlin, https://doi.org/10.14279/depositonce-9125, 2019.

Balidakis, K., Nilsson, T., Zus, F., Glaser, S., Heinkelmann, R., Deng, Z., and Schuh, H.: Estimating integrated water vapor trends from VLBI, GPS, and numerical weather models: Sensitivity to tropospheric parameterization, J GEOPHYS RES-ATMOS, 123, 6356–6372, 2018.

Bock, O., Willis, P., Lacarra, M., and Bosser, P.: An inter-comparison of zenith tropospheric delays derived from DORIS and GPS data, Advances in Space Research, 46, 1648–1660, 2010.

Böhm, J., Werl, B., and Schuh, H.: Troposphere mapping functions for GPS and VLBI from ECMWF operational analysis data, J GEOPHYS RES, 111, 1–9, 2006.

Chen, G. and Herring, T.: Effects of atmospheric azimuthal asymmetry on the analysis of space geodetic data, J GEOPHYS RES-SOL EA, 102, 20 489–20 502, 1997.

Dach, R., Lutz, S., Walser, P., and Fridez, P. e.: Bernese GNSS Software Version 5.2, University of Bern, Bern Open Publishing, https://doi.org/10.7892/BORIS.72297, 2015.

Dach, R., Schaer, S., Arnold, D., Kalarus, M. S., Prange, L., Stebler, P., Villiger, A., and Jäggi, A.: CODE final product series for the IGS, Astronomical Institute, University of Bern, https://doi.org/10.7892/BORIS.75876.4, 2020.

Dousa, J. and Vaclavovic, P.: Real-time zenith tropospheric delays in support of numerical weather prediction applications, Advances in Space Research, 53, 1347–1358, 2014.

Heinkelmann, R., Willis, P., Deng, Z., Dick, G., Nilsson, T., Soja, B., Zus, F., Wickert, J., and Schuh, H.: Multi-technique comparison of atmospheric parameters at the DORIS co-location sites during CONT14, Advances in Space Research, 58, 2758–2773, 2016.

Hersbach, H., Bell, B., Berrisford, P., Hirahara, S., Horányi, A., Muñoz-Sabater, J., Nicolas, J., Peubey, C., Radu, R., Schepers, D., et al.: The ERA5 global reanalysis, Q J R Meteorol Soc, 146, 1999–2049, 2020.

Hobiger, T. and Otsubo, T.: Combination of GPS and VLBI on the observation level during CONT11—common parameters, ties and inter-technique biases, J GEODESY, 88, 1017–1028, 2014.

IGS: IGS site guidelines, https://kb.igs.org/hc/en-us/articles/202011433-Current-IGS-Site-Guidelines, 2019.

Kitpracha, C., Balidakis, K., Heinkelmann, R., and Schuh, H.: Assessment on atmospheric parameters at co-location sites, in: EGU General Assembly Conference Abstracts, p. 6517, 2020.

Kitpracha, C., Heinkelmann, R., Ramatschi, M., Balidakis, K., Männel, B., and Schuh, H.: The GNSS co-location experiment at Potsdam, GFZ Data Services, https://doi.org/https://doi.org/10.5880/GFZ.1.1.2021.005, 2021.

Krügel, M., Thaller, D., Tesmer, V., Rothacher, M., Angermann, D., and Schmid, R.: Tropospheric parameters: combination studies based on homogeneous VLBI and GPS data, J GEODESY, 81, 515–527, 2007.

Landskron, D. and Böhm, J.: VMF3/GPT3: refined discrete and empirical troposphere mapping functions, J GEODESY, 92, 349–360, 2018.

Männel, B., Thaller, D., Rothacher, M., Böhm, J., Müller, J., Glaser, S., Dach, R., Biancale, R., Bloßfeld, M., Kehm, A., Pinzón, I. H., Hofmann, F., Andritsch, F., Coulot, D., and Pollet, A.: Recent Activities of the GGOS Standing Committee on Performance Simulations

https://doi.org/10.5194/amt-2022-238
Preprint. Discussion started: 29 August 2022

and Architectural Trade-Offs (PLATO), in: International Symposium on Advancing Geodesy in a Changing World, edited by Freymueller, J. T. and Sánchez, L., pp. 161–164, Springer International Publishing, Cham, 2019.

Nilsson, T., Böhm, J., Wijaya, D. D., Tresch, A., Nafisi, V., and Schuh, H.: Path Delays in the Neutral Atmosphere, pp. 73–136, Springer Berlin Heidelberg, Berlin, Heidelberg, https://doi.org/10.1007/978-3-642-36932-2_3, 2013.

Ning, T. and Elgered, G.: Trends in the atmospheric water vapor content from ground-based GPS: The impact of the elevation cutoff angle, IEEE Journal of Selected Topics in Applied Earth Observations and Remote Sensing, 5, 744–751, 2012.

Petit, G. and Luzum, B.: IERS conventions (2010), Tech. rep., Bureau International des Poids et mesures sevres (France), 2010.

Pinzón, I. H. and Rothacher, M.: Assessment of local GNSS baselines at co-location sites, J GEODESY, 92, 1079–1095, 2018.

Plag, H.-P., Rothacher, M., Pearlman, M., Neilan, R., and Ma, C.: The global geodetic observing system, in: Advances in Geosciences: Volume 13: Solid Earth (SE), pp. 105–127, World Scientific, 2009.

Pollet, A., Coulot, D., Bock, O., and Nahmani, S.: Comparison of individual and combined zenith tropospheric delay estimations during CONT08 campaign, J GEODESY, 88, 1095–1112, 2014.

Ramatschi, M., Bradke, M., Nischan, T., and Männel, B.: GNSS data of the global GFZ tracking network, https://doi.org/10.5880/GFZ.1.1.2020.001, 2019.

Ray, J. and Altamimi, Z.: Evaluation of co-location ties relating the VLBI and GPS reference frames, J GEODESY, 79, 189–195, 2005.

Rebischung, P. and Schmid, R.: IGS14/igs14. atx: a new framework for the IGS products, in: AGU Fall Meeting 2016, 2016.

Rothacher, M., Angermann, D., Artz, T., Bosch, W., Drewes, H., Gerstl, M., Kelm, R., König, D., König, R., Meisel, B., Müller, H., Nothnagel, A., Panafidina, N., Richter, B., Rudenko, S., Schwegmann, W., Seitz, M., Steigenberger, P., Tesmer, S., Tesmer, V., and Thaller, D.: GGOS-D: Homogeneous reprocessing and rigorous combination of space geodetic observations, J GEODESY, 85, 679–705, https://doi.org/10.1007/s00190-011-0475-x, 2011.

Schmid, R.: Zur Kombination von VLBI und GNSS, DGK, Reihe C, Heft 636, Verlag der Bayerischen Akademie der Wissenschaften, ISBN 978-3-7696-5048-8, 2009.

Schuh, H. and Behrend, D.: VLBI: A fascinating technique for geodesy and astrometry, J GEODYN, 61, 68–80, 2012.

Steigenberger, P., Hugentobler, U., Schmid, R., Hessels, U., Klügel, T., and Seitz, M.: GPS-specific local effects at the Geodetic Observatory Wettzell, in: Reference frames for applications in geosciences, pp. 125–130, Springer, 2013.

Teke, K., Böhm, J., Nilsson, T., Schuh, H., Steigenberger, P., Dach, R., Heinkelmann, R., Willis, P., Haas, R., García-Espada, S., et al.: Multi-technique comparison of troposphere zenith delays and gradients during CONT08, J GEODESY, 85, 395, 2011.

Teke, K., Nilsson, T., Böhm, J., Hobiger, T., Steigenberger, P., García-Espada, S., Haas, R., and Willis, P.: Troposphere delays from space geodetic techniques, water vapor radiometers, and numerical weather models over a series of continuous VLBI campaigns, J GEODESY, 87, 981–1001, 2013.

Wilgan, K., Dick, G., Zus, F., and Wickert, J.: Towards operational multi-GNSS tropospheric products at GFZ Potsdam, Atmos Meas Tech, 15, 21–39, https://doi.org/10.5194/amt-15-21-2022, 2022.